

Contrastive Vicinal Space for Unsupervised Domain Adaptation

Jaemin Na¹, Dongyoon Han², Hyung Jin Chang³, and Wonjun Hwang¹

¹Ajou University, Korea, ²NAVER AI Lab, ³University of Birmingham, UK

osial46@ajou.ac.kr, dongyoon.han@navercorp.com, h.j.chang@bham.ac.uk, wjhwang@ajou.ac.kr

Abstract

Utilizing vicinal space between the source and target domains is one of the recent unsupervised domain adaptation approaches. However, the problem of the equilibrium collapse of labels, where the source labels are dominant over the target labels in the predictions of vicinal instances, has never been addressed. In this paper, we propose an instance-wise minimax strategy that minimizes the entropy of high uncertainty instances in the vicinal space to tackle it. We divide the vicinal space into two subspaces through the solution of the minimax problem: contrastive space and consensus space. In the contrastive space, inter-domain discrepancy is mitigated by constraining instances to have contrastive views and labels, and the consensus space reduces the confusion between intra-domain categories. The effectiveness of our method is demonstrated on the public benchmarks, including Office-31, Office-Home, and VisDA-C, which achieve state-of-the-art performances. We further show that our method outperforms current state-of-the-art methods on PACS, which indicates our instance-wise approach works well for multi-source domain adaptation as well.

1. Introduction

Unsupervised domain adaptation (UDA) aims to adapt a model trained on a labeled source domain to an unlabeled target domain. One of the most important problems to solve in UDA is the domain shift [39] (*i.e.*, distribution shift) problem. The domain shift arises from the change in the data distribution between the training domain (*i.e.*, source domain) of an algorithm and the test domain encountered in a practical application (*i.e.*, target domain). Although recent UDA studies [30, 47, 52] have shown encouraging results, a large domain shift is still a significant obstacle.

One recent paradigm to address the large domain shift problems is to leverage intermediate domains between the source and target domains instead of direct domain adaptation. Latest studies [6, 13] inspired by generative adversarial networks [14] (GANs) generate instances of intermediate domains to bridge the source and target do-

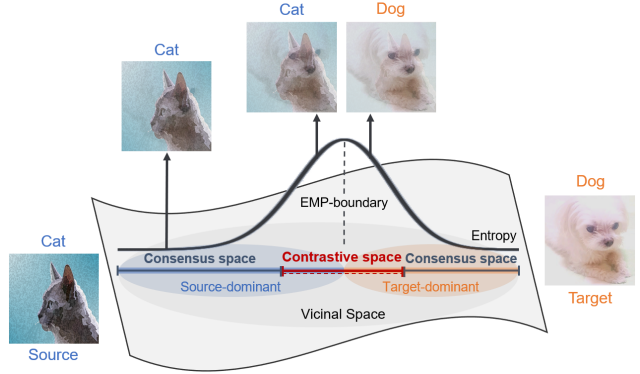


Figure 1. **Overview.** Vicinal space between the source and target domains is divided into contrastive space and consensus space. Our methodology alleviates inter-domain discrepancy in the contrastive space and simultaneously resolves intra-domain categorical confusion in the consensus space.

main. To avoid time-consuming generative methods, [3, 8] learns domain-invariant representations by borrowing only the concept of adversarial training. Meanwhile, with the development of data augmentation techniques, many approaches have emerged built on data augmentation to construct the intermediate spaces. Recent studies [30, 46, 49] have shown promising results with grafting the Mixup augmentation [53] to the domain adaptation task. These studies use inter-domain mixup to efficiently overcome the domain shift problem by utilizing vicinal instances between the source and target domains. However, none of them considers leveraging the predictions of the vicinal instances in the perspective of self-training [22].

Self-training is the straightforward approach that uses self-predictions of a model to train itself. Semi-supervised learning methods [22, 33] leverage a models' predictions on unlabeled data to obtain additional information used during training as their supervision. In particular, unsupervised domain adaptation methods [15, 35, 40] have shown that the self-training method (*i.e.*, Pseudo-label [22]) can play an important role in alleviating the domain shift problem.

In this work, we introduce a new **Contrastive Vicinal**

space-based (CoVi) algorithm that leverages vicinal instances from the perspective of self-training [22]. We utilize top- k predictions on vicinal instances to obtain valuable target supervisions. To efficiently use the vicinal spaces, we investigate the vicinal instances and their corresponding predictions. We empirically observe that the source label is generally dominant over the target label before applying domain adaptation. In other words, one-hot predictions of the vicinal instances with the same ratio of source and target instances are much more likely to be source labels. Even when the proportions of target instances are high (e.g., target-dominant instances), they are likely to be represented by the source labels (e.g., source-dominant labels). We define this phenomenon as the **equilibrium collapse of labels** between vicinal instances. Furthermore, we observe that the entropy of the predictions is maximum at the boundary where the equilibrium collapse of labels occurs. We also discover that this result comes from the confusion between source and target instances. With these observations, we aim to find and address the points where the entropy is maximized between the vicinal instances. Inspired by the minimax strategy [10], we present *EMP-Mixup*, which minimizes the entropy for the *entropy maximization point (EMP)*. Our *EMP-Mixup* adaptively adjusts the Mixup ratio according to the combinations of source and target instances.

Taking advantage of the *EMP-Mixup*, we use EMP as a boundary (i.e., *EMP-boundary*) to divide the vicinal space into source-dominant and target-dominant spaces. Moreover, as depicted in Figure 1, we constrain the **contrastive space** around *EMP-boundary* so that the instances of source-dominant and target-dominant spaces have contrastive views of each other. In addition, from the perspective of self-training, we obtain top-2 contrastive labels corresponding to the predictions of the contrastive views. Considering that vicinal instances are constructed only with the source and target instances, we only focus on the top-2 predictions. In the contrastive space, the source-dominant instances have source labels as their first labels (i.e., *source-dominant labels*) and target labels as their second labels (i.e., *target-recessive labels*). On the other hand, target-dominant instances have *target-dominant labels* and *source-recessive labels*. Therefore, this allows for swapping of the predicted top-2 contrastive labels from the contrastive views to learn through self-predictions from the other views.

Unlike previous studies that are reluctant to use an excessively target-biased space due to the high uncertainty, we define and take advantage of this space as **consensus space**. In contrast to our attention on mitigating inter-domain discrepancy in contrastive space, we are more concerned with resolving categorical uncertainties within intra-domain in consensus space. We reduce the uncertainty of predictions on target instances by utilizing the multiple source instances in vicinal space. Here, we exploit the source instances to

perturb to predictions of target instances. Through this, our target-label consensus ensures more consistent and robust predictions for the target instances.

We perform extensive ablation studies for a detailed analysis of the proposed methods. In particular, we achieve comparable performance to the recent state-of-the-art methods in standard unsupervised domain adaptation benchmarks such as Office-31 [34], Office-Home [44], and VisDA-C [32]. Furthermore, we validate the superiority of our instance-wise approach on the PACS [24] dataset for multi-source domain adaptation.

Overall, we make the following contributions:

- This is the first study in UDA to leverage the vicinal space from the perspective of self-training. We shed light on the problem of the equilibrium collapse of labels in the vicinal space and propose a minimax strategy to handle it.
- We alleviate inter-domain and intra-domain confusions by dividing the vicinal space into contrastive and consensus spaces.
- Our method achieves state-of-the-art performance and is further validated through extensive ablation studies.

2. Related Work

Unsupervised Domain Adaptation. One of the representative domain adaptation methods [11, 12, 48] is learning a domain invariant representation or aligning the global distribution between the source and target domains. Of particular interest, Xie *et al.* [48] presented a moving semantic transfer network that aligns labeled source centroid and pseudo-labeled target centroid to learn semantic representations for unlabeled target data. Following [5, 15, 30], we adopt this simple but efficient method as our baseline.

Our work is also related to the domain adaptation approaches that consider the inter-domain and intra-domain gap together. Kang *et al.* [21] proposed to minimize the intra-class discrepancy and maximize the inter-class discrepancy to perform class-aware domain alignment. Recently, Pan *et al.* [31] presented a semantic segmentation methodology that minimizes both inter-domain and intra-domain gaps. Unlike the previous methods, we introduce a practical approach that consists of contrastive space for inter-domain and consensus space for intra-domain space.

Mixup Augmentation. Mixup [53] is a data-agnostic and straightforward augmentation using a linear interpolation between two data instances. The Mixup augmentation has been applied to various tasks and shown to improve the robustness of neural networks. The recent semi-supervised learning methods [1, 2, 41] efficiently utilized Mixup to leverage unlabeled data. Meanwhile, several domain adaptation methods [30, 46, 49] with Mixup were proposed to alleviate the domain-shift problem successfully. Xu *et al.* [49] and Wu *et al.* [46] showed promising results using inter-domain Mixup between source and target

domains. Recently, Na *et al.* [30] achieved a significant performance gain by using two networks trained with two fixed Mixup ratios.

Moreover, the latest studies [16, 28, 54] suggested adaptive Mixup techniques instead of using manually designed interpolation policies. For example, Zhu *et al.* [54] introduced a more advanced interpolation technique that seeks the Wasserstein barycenter between two instances. This is then generalized to propose an adaptive Mixup. Mai *et al.* [28] introduced a meta-learning-based optimization strategy for dynamically learning the interpolation policy in semi-supervised learning. However, note that unsupervised domain adaptation methods still count on hand-tuned or random interpolation policies.

In unsupervised domain adaptation, relying on the random interpolation policy has the following limitations. First, reducing the discrepancy of instance-level between the source and target domains is as important as alleviating the global discrepancy. This is because the degree of domain shift is different from instance to instance, even if they belong to the same domain. However, the traditional Mixup does not consider the characteristics of instance-level at all. Second, extremely target-biased Mixup can negatively affect learning, as noted in Na *et al.* [30], due to the practice of using inaccurate target labels as pseudo-labels. From these perspectives, in this work, we derive the Mixup ratio according to the convex combinations of source and target instances instead of using a random interpolation policy.

3. Methodology

We introduce three techniques of CoVi to leverage the vicinal space between the source and target domains: EMP-Mixup, contrastive views and labels, and a label-consensus. An overall depiction of CoVi is in Figure 2.

3.1. Preliminaries

Notation. We denote a mini-batch of m -images as \mathcal{X} , corresponding labels as \mathcal{Y} , and extracted features from \mathcal{X} as \mathcal{Z} . Specifically, $\mathcal{X}_S \subset \mathbb{R}^{m \times i}$ and $\mathcal{Y}_S \subset \{0, 1\}^{m \times n}$ denote the mini-batches of source instances and their corresponding one-hot labels, respectively. Here, n denotes the number of classes and $i = c \cdot h \cdot w$, where c denotes the channel size, and h and w denote the height and width of the image instances, respectively. Similarly, the mini-batch of unlabeled target instances is $\mathcal{X}_T \subset \mathbb{R}^{m \times i}$. Our model consists of the following subcomponents: an *encoder* f_θ , a *classifier* h_θ , and an *EMP-learner* g_ϕ .

Mixup. The *Mixup* augmentation [53] based on the Vicinal Risk Minimization (VRM) [7] principle exploits virtual instances constructed with the linear interpolation of two instances. These vicinal instances can benefit unsupervised domain adaptation (UDA), which has no target domain la-

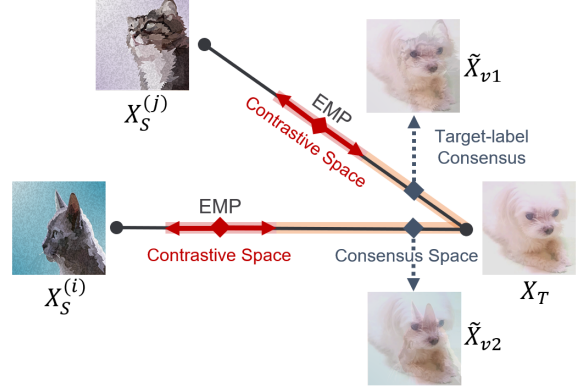


Figure 2. **Schematic illustration of CoVi.** The *EMP-Mixup* finds the most confusing point (*i.e.*, EMP) among vicinal instances. CoVi then learns through top- k contrastive predictions from contrastive views in the contrastive space determined by the EMP. In the consensus space, we achieve a target-label consensus with perturbations of the source instances.

bels. We define the inter-domain Mixup applied between the source and target domains as follows:

$$\begin{aligned}\tilde{\mathcal{X}}_\lambda &= \lambda \cdot \mathcal{X}_S + (1 - \lambda) \cdot \mathcal{X}_T \\ \tilde{\mathcal{Y}}_\lambda &= \lambda \cdot \mathcal{Y}_S + (1 - \lambda) \cdot \hat{\mathcal{Y}}_T,\end{aligned}\quad (1)$$

where $\hat{\mathcal{Y}}_T$ denotes the pseudo labels of the target instances and $\lambda \in [0, 1]$ is the Mixup ratio. Then, the empirical risk for vicinal instances in the inter-domain Mixup is defined as follows:

$$\mathcal{R}_\lambda = \frac{1}{m} \sum_{i=1}^m \mathcal{H}[h(f(\tilde{\mathcal{X}}_\lambda^{(i)})), \tilde{\mathcal{Y}}_\lambda^{(i)}], \quad (2)$$

where \mathcal{H} is a standard cross-entropy loss.

3.2. EMP-Mixup

In the vicinal space between the source and target domains, we make striking observations on unsupervised domain adaptation.

Observation 1. “The labels of the target domain are relatively recessive compared to the source domain labels.”

We investigate the dominance of the predicted top-1 labels between the source and target instances in vicinal instances. We find the label dominance is balanced when the labels of both the source and target domains are provided (*i.e.*, supervised learning). In this case, the top-1 label of the vicinal instance is determined by the instance occupying a relatively larger proportion. However, in the UDA, where the label of the target domain is not given, the balance of label dominance is broken (*i.e.*, equilibrium collapse of labels). Indeed, we discover that source labels frequently represent vicinal instances with a higher proportion of target instances than source instances.

Observation 2. “Depending on the convex combinations of source and target instances, the label dominance is changed.”

Next, we have observed that the label dominance is being altered according to the convex combinations of instances. In addition, we have discovered that the entropy of the prediction is maximum at the point where the label dominance changes because the source and target instances become most confusing at this point (see Figures 4 and 5).

Based on these findings, we aim to capture and mitigate the most confusing points. Inspired by [10, 14, 29], we introduce a minimax strategy to break through the worst-case risk [10] among the vicinal instances between the source and target domains. We minimize the worst risk by finding the **entropy maximization point (EMP)** among the vicinal instances. In order to estimate the EMPs, we introduce a small network, *EMP-learner*. This network aims to generate Mixup ratios that maximize the entropy of the encoder f_θ (e.g., *ResNet*) followed by a classifier h_ϕ .

Given \mathcal{X}_S and \mathcal{X}_T , we obtain the instance features $\mathcal{Z}_S = f_\theta(\mathcal{X}_S)$ and $\mathcal{Z}_T = f_\theta(\mathcal{X}_T)$ from the encoder f_θ . Then, we pass the concatenated features $\mathcal{Z}_S \oplus \mathcal{Z}_T$ to the *EMP-learner* g_ϕ . Then, the *EMP-learner* produces the entropy maximization ratio λ^* that maximizes the entropy of the encoder f_θ . Formally, the Mixup ratios for our *EMP-Mixup* are defined as follows:

$$\lambda^* = \arg \max_{\lambda \in [0,1]} \mathcal{H}[h_\phi(f_\theta(\tilde{\mathcal{X}}_\lambda))], \quad (3)$$

where $\lambda = g_\phi(\mathcal{Z}_S \oplus \mathcal{Z}_T)$ and \mathcal{H} is the entropy loss. Finally, we design the objective function for *EMP-learner* to **maximize the entropy** as follows:

$$\mathcal{R}_\lambda(\phi) = \frac{1}{m} \sum_{i=1}^m \mathcal{H}[h(f(\tilde{\mathcal{X}}_\lambda^{(i)}))], \quad (4)$$

where \mathcal{H} is the entropy loss. Note that we only update the parameter ϕ of the *EMP-learner*, not the parameter θ of the encoder and the classifier.

With the worst-case ratio λ^* , *EMP-Mixup* **minimizes the worst-case risk** on vicinal instances as follows:

$$\mathcal{R}_{\lambda^*}(\theta) = \frac{1}{m} \sum_{i=1}^m \mathcal{H}[h(f(\tilde{\mathcal{X}}_{\lambda^*}^{(i)})), \tilde{\mathcal{Y}}_{\lambda^*}^{(i)}], \quad (5)$$

where \mathcal{H} is the standard cross-entropy loss.

It is worth noting that our $\lambda^* = [\lambda_1, \dots, \lambda_m]$ has different optimized ratios according to the combinations of the source and target instances within a mini-batch. Finally, *EMP-Mixup* minimizes the risk of vicinal instances from the viewpoint of the worst-case risk. The overall objective functions are defined as follows:

$$\mathcal{R}_{emp} = \mathcal{R}_{\lambda^*}(\theta) - \mathcal{R}_\lambda(\phi). \quad (6)$$

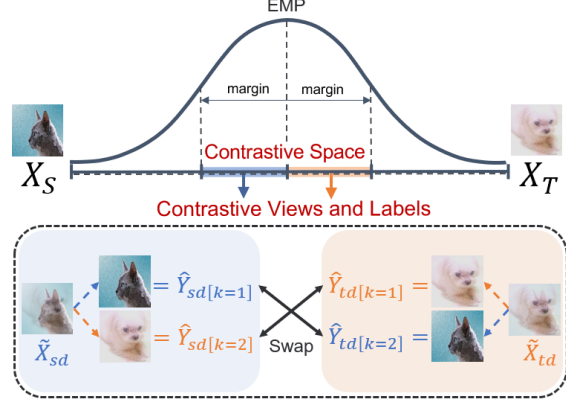


Figure 3. **Contrastive views and labels.** (i) The **contrastive views** consist of a source-dominant view $\tilde{\mathcal{X}}_{sd}$ and a target-dominant view $\tilde{\mathcal{X}}_{td}$. (ii) The **contrastive labels** comprise the source-dominant label and target-recessive label from the top-2 predictions in the contrastive view $\tilde{\mathcal{X}}_{sd}$ (and vice versa).

3.3. Contrastive Views and Labels

Observation 3. “The dominant/recessive labels of the vicinal instances are switched at the EMP.”

Looking back to the previous observations, the label dominance changes according to the convex combination of instances, and the point of change is the EMP. In other words, with the EMP as a boundary (i.e., *EMP-boundary*), the dominant/recessive label is switched between the source and target domains. Hence, vicinal instances around the *EMP-boundary* should have source and target labels as their top-2 labels.

These observations and analyses lead us to design the concepts of contrastive views and contrastive labels. Owing to the *EMP-boundary*, we divide the vicinal space into a source-dominant and target-dominant space, as described in Figure 3. Consequently, the source-dominant instances $\tilde{\mathcal{X}}_{sd}$ and target-dominant instances $\tilde{\mathcal{X}}_{td}$ have **contrastive views** of each other. Specifically, we constrain the source-dominant and target-dominant spaces of the contrastive space to $\lambda^* - \omega < \lambda_{sd} < \lambda^*$ and $\lambda^* < \lambda_{td} < \lambda^* + \omega$, respectively. Here, ω is the margin of the ratio from the *EMP-boundary*.

From the contrastive views, we focus on the top-2 labels for each prediction because we are only interested in the classes that correspond to the source and target instances, not the other classes. Here, we define a set of top-2 one-hot labels within a mini-batch as $\hat{\mathcal{Y}}_{[k=1]}$ and $\hat{\mathcal{Y}}_{[k=2]}$. Unlike a general Mixup that uses pure source and target labels (see Eq. 1), we directly exploit the predicted labels from vicinal instances. In this case, for example, the labels for the instances of the target-dominant space are constructed as follows:

$$\hat{\mathcal{Y}}_{td} = \lambda_{td} \cdot \hat{\mathcal{Y}}_{td[k=1]} + (1 - \lambda_{td}) \cdot \hat{\mathcal{Y}}_{td[k=2]}. \quad (7)$$

Furthermore, we expand on this and propose a new concept of **contrastive labels**. We constrain the top-2 labels from our contrastive views as follows:

- $\hat{\mathcal{Y}}_{sd[k=1]}$ from $\tilde{\mathcal{X}}_{sd}$ and $\hat{\mathcal{Y}}_{td[k=2]}$ from $\tilde{\mathcal{X}}_{td}$ must be equal, as the predictions of the source instances.
- Similarly, $\hat{\mathcal{Y}}_{sd[k=2]}$ must be equal to $\hat{\mathcal{Y}}_{td[k=1]}$, as for the predictions of the target instances.

In other words, the dominant label $\hat{\mathcal{Y}}_{sd[k=1]}$ of $\tilde{\mathcal{X}}_{sd}$ and the recessive label $\hat{\mathcal{Y}}_{td[k=2]}$ of $\tilde{\mathcal{X}}_{td}$ must be the same as the source labels and vice versa. It is worth noting that our contrastive constraints are instance-level constraints that must be satisfied between any instances, regardless of the class category.

Consequently, we swap the top-2 contrastive labels between two contrastive views to learn from the predictions of another view. According to the constraints, Eq.7 still holds when even we exchange the contrastive labels. Finally, the objective for our contrastive loss in target-dominant space is defined as follows:

$$\mathcal{R}_{td}(\theta) = \frac{1}{m} \sum_{i=1}^m \mathcal{H}[h(f(\tilde{\mathcal{X}}_{td}^{(i)})), \hat{\mathcal{Y}}_{td}^{(i)}], \quad (8)$$

where $\hat{\mathcal{Y}}_{td} = \lambda_{td} \cdot \hat{\mathcal{Y}}_{sd[k=2]} + (1 - \lambda_{td}) \cdot \hat{\mathcal{Y}}_{sd[k=1]}$.

Similarly, we define $\mathcal{R}_{sd}(\theta)$ in the source-dominant space and omit it for clarity. The overall objective functions for contrastive loss are defined as follows:

$$\mathcal{R}_{ct} = \mathcal{R}_{td}(\theta) + \mathcal{R}_{sd}(\theta). \quad (9)$$

3.4. Label Consensus

Even though the confusion between the source and target instances is crucial in the contrastive space, outside of the contrastive space (*i.e.*, **consensus space**), we need to pay more attention to the uncertainty of predictions within the intra-domain than inter-domain instances (see Figure 6). Here, we exploit the multiple source instances to impose perturbations to target predictions rather than classification information.

We construct two randomly shuffled versions of the source instances within a mini-batch. We then apply Mixup with a single target mini-batch to obtain two different perturbed views v_1 and v_2 . We compute two softmax probabilities from the two perturbed instances $\tilde{\mathcal{X}}_{v_1}$ and $\tilde{\mathcal{X}}_{v_2}$ using an encoder, followed by a classifier. Finally, we aggregate the softmax probabilities and yield a one-hot prediction $\hat{\mathcal{Y}}$.

We accomplish **target-label consensus** on predicting one target-dominant instance perturbed by the two different source instances through the label $\hat{\mathcal{Y}}$. Learning two versions of perturbed instances to a single target label allows us to focus on the target domain category rather than the source

domain category. We empirically constrain the consensus space to be close to the target domain. The objective for label consensus on target instances can be defined as follows:

$$\mathcal{R}_{cs}(\theta) = \frac{1}{m} \sum_{i=1}^m [\mathcal{H}(h(f(\tilde{\mathcal{X}}_{v_1}^{(i)})), \hat{\mathcal{Y}}^{(i)}) + \mathcal{H}(h(f(\tilde{\mathcal{X}}_{v_2}^{(i)})), \hat{\mathcal{Y}}^{(i)})], \quad (10)$$

where \mathcal{H} is the cross-entropy loss.

Note that this approach is also applicable to source-dominant space, but we exclude it from the final loss as it does not significantly affect the performance.

4. Experiments

We evaluated our method on four popular benchmarks including *Office-31*, *Office-Home*, *VisDA-C*, and *PACS*. In particular, the *PACS* is a multi-source domain adaptation dataset.

- **Office-31** [34] contains 31 categories and 4,110 images in three domains: Amazon (A), Webcam (W), and DSLR (D). We verify our methodology in six domain adaptation tasks.

- **Office-Home** [44] consists of 64 categories and 15,500 images in four domains: Art (Ar), Clipart (CI), Product (Pr), and Real-World (Rw).

- **VisDA-C** [32] is a large-scale dataset for synthetic-to-real domain adaptation across 12 categories. It contains 152,397 synthetic images for the source domain and 55,388 real-world images for the target domain.

- **PACS** [24] is organized into seven categories with 9,991 images in four domains: Photo (P), Art Painting (A), Cartoon (C), and Sketch (S). We evaluate our method on the PACS dataset for multi-source domain adaptation.

4.1. Experimental Setups

Following the standard UDA protocol [11, 12], we utilize labeled source data and unlabeled target data. We exploit ResNet-50 [17, 18] for Office-31 and Office-home, and ResNet-101 for VisDA-C. For multi-source domain adaptation, we use ResNet-18 for PACS. We use stochastic gradient descent (SGD) optimization in all our experiments. For our contrastive loss and label consensus loss, we follow the confidence masking policy of FixBi [30] that adaptively changes according to the sample mean and standard deviation across all mini-batches. Meanwhile, we design the *EMP-learner* by simply using four convolutional layers, regardless of the dataset. More detailed information is provided in the supplementary materials.

4.2. Comparison with the state-of-the-art methods

We validate our method with state-of-the-art methods on three public benchmarks. We report the accuracy of Office-31, Office-Home, and VisDA-C.

Office-31. In Table 1, we show the comparative performance on ResNet-50. We achieve 91.8% accuracy, which

Method	A→W	D→W	W→D	A→D	D→A	W→A	Avg
MSTN* (Baseline) [48]	91.3	98.9	100.0	90.4	72.7	65.6	86.5
DWL (CVPR'21) [47]	89.2	99.2	100.0	91.2	73.1	69.8	87.1
DMRL (ECCV'20) [46]	90.8±0.3	99.0±0.2	100.0±0.0	93.4±0.5	73.0±0.3	71.2±0.3	87.9
ILA-DA (CVPR'21) [38]	95.72	99.25	100.0	93.37	72.10	75.40	89.3
MCC (ECCV'20) [20]	95.5±0.2	98.6±0.1	100.0±0.0	94.4±0.3	72.9±0.2	74.9±0.3	89.4
GSDA (CVPR'20) [19]	95.7	99.1	100	94.8	73.5	74.9	89.7
SRDC (CVPR'20) [42]	95.7±0.2	99.2±0.1	100.0±0.0	95.8±0.2	76.7±0.3	77.1±0.1	90.8
RSDA (CVPR'20) [15]	<u>96.1±0.2</u>	<u>99.3±0.2</u>	100.0±0.0	<u>95.8±0.3</u>	77.4±0.8	<u>78.9±0.3</u>	91.1
FixBi (CVPR'21) [30]	<u>96.1±0.2</u>	<u>99.3±0.2</u>	100.0±0.0	95.0±0.4	78.7±0.5	79.4±0.3	91.4
CoVi (Ours)	97.6±0.2	99.3±0.1	100.0±0.0	98.0±0.3	<u>77.5±0.3</u>	78.4±0.3	91.8

Table 1. Accuracy (%) on Office-31 for unsupervised domain adaptation (ResNet-50). The best accuracy is indicated in bold, and the second-best accuracy is underlined. * Reproduced by [5].

Method	Ar→Cl	Ar→Pr	Ar→Rw	Cl→Ar	Cl→Pr	Cl→Rw	Pr→Ar	Pr→Cl	Pr→Rw	Rw→Ar	Rw→Cl	Rw→Pr	Avg
MSTN* (Baseline) [48]	49.8	70.3	76.3	60.4	68.5	69.6	61.4	48.9	75.7	70.9	55	81.1	65.7
AADA (ECCV'20) [50]	54.0	71.3	77.5	60.8	70.8	71.2	59.1	51.8	76.9	71.0	57.4	81.8	67.0
ETD (CVPR'20) [25]	51.3	71.9	85.7	57.6	69.2	73.7	57.8	51.2	79.3	70.2	57.5	82.1	67.3
GSDA (CVPR'20) [19]	61.3	76.1	79.4	65.4	73.3	74.3	65	53.2	80	72.2	60.6	83.1	70.3
GVB-GD (CVPR'20) [8]	57	74.7	79.8	64.6	74.1	74.6	65.2	55.1	81	74.6	59.7	84.3	70.4
TCM (ICCV'21) [52]	58.6	74.4	79.6	64.5	74.0	75.1	64.6	56.2	80.9	74.6	60.7	84.7	70.7
RSDA (CVPR'20) [15]	53.2	<u>77.7</u>	<u>81.3</u>	66.4	74	76.5	<u>67.9</u>	53	82	75.8	57.8	85.4	70.9
SRDC (CVPR'20) [42]	52.3	76.3	81	69.5	76.2	<u>78</u>	68.7	53.8	81.7	76.3	57.1	85	71.3
MetaAlign (CVPR'21) [45]	59.3	76.0	80.2	65.7	74.7	75.1	65.7	56.5	81.6	74.1	61.1	85.2	71.3
FixBi (CVPR'21) [30]	58.1	77.3	80.4	67.7	<u>79.5</u>	78.1	65.8	<u>57.9</u>	81.7	<u>76.4</u>	<u>62.9</u>	86.7	72.7
CoVi (Ours)	58.5	78.1	80.0	<u>68.1</u>	80.0	77.0	66.4	60.2	82.1	76.6	63.6	<u>86.5</u>	73.1

Table 2. Accuracy (%) on Office-Home for unsupervised domain adaptation (ResNet-50). The best accuracy is indicated in bold, and the second-best accuracy is underlined. * Reproduced by [15].

Method	aero	bicycle	bus	car	horse	knife	motor	person	plant	skate	train	truck	Avg
MSTN* (Baseline) [48]	89.3	49.5	74.3	67.6	90.1	16.6	93.6	70.1	86.5	40.4	83.2	18.5	65.0
DMRL (ECCV'20) [46]	-	-	-	-	-	-	-	-	-	-	-	-	75.5
TCM (ICCV'21) [52]	-	-	-	-	-	-	-	-	-	-	-	-	75.8
DWL (CVPR'21) [47]	90.7	80.2	86.1	67.6	92.4	81.5	86.8	78.1	90.6	57.1	85.6	28.7	77.1
CGDM (ICCV'21) [9]	93.4	82.7	73.2	68.4	92.9	94.5	88.7	82.1	93.4	82.5	86.8	<u>49.2</u>	82.3
STAR (CVPR'20) [27]	95	84	84.6	73	91.6	91.8	85.9	78.4	94.4	84.7	87	42.2	82.7
CAN (CVPR'19) [21]	97	<u>87.2</u>	82.5	74.3	97.8	96.2	90.8	80.7	<u>96.6</u>	96.3	87.5	59.9	<u>87.2</u>
FixBi (CVPR'21) [30]	96.1	87.8	90.5	90.3	<u>96.8</u>	<u>95.3</u>	<u>92.8</u>	88.7	97.2	<u>94.2</u>	<u>90.9</u>	25.7	<u>87.2</u>
CoVi (Ours)	<u>96.8</u>	85.6	<u>88.9</u>	<u>88.6</u>	97.8	93.4	91.9	<u>87.6</u>	96.0	93.8	93.6	48.1	88.5

Table 3. Accuracy (%) on VisDA-C for unsupervised domain adaptation (ResNet-101). The best accuracy is indicated in bold, and the second-best accuracy is underlined. * Reproduced by [5].

outperforms other state-of-the-art methods. Our method performs best in four out of six situations, *e.g.*, A→W, D→W, W→D, and A→D tasks. In particular, in A→W and A→D, the performance improvement of recent methods is stagnant but our method shows a significant performance gain. Compared to the DMRL [46] and FixBi [30], which utilize Mixup [53], we also obtain better performance.

Office-Home. Table 2 demonstrates the comparison results on the Office-Home dataset based on ResNet-50. Our method achieves the best performance in 50% of the tasks and is the first feat to break the 73% barrier. In particular, we achieve over 10% higher performance from the baseline in Cl→Pr and Pr→Cl. In addition, our method outperforms MetaAlign [45], which uses meta-learning schemes, and FixBi [30], which ensembles the networks' outputs.

VisDA-C. In Table 3, we validate our method on a large visual domain adaptation challenge dataset with ResNet-101. Our method achieves a performance improvement of over 23% compared to the baseline MSTN [48]. In addition, our method shows better performance than the mixup-based DMRL [46] and FixBi [30]. Our method outperforms the state-of-the-art methods with an accuracy of 88.5%. We could not achieve the best accuracy across all categories due to the poor accuracy of the baseline (65.0%), yet the overall score supports the effectiveness of our method.

4.3. Ablation Studies and Discussions

Analysis of EMP. We provide visual examples of the predictions of vicinal instances using Grad-CAM [36] in Figure 4. Grad-CAM highlights class-discriminative region

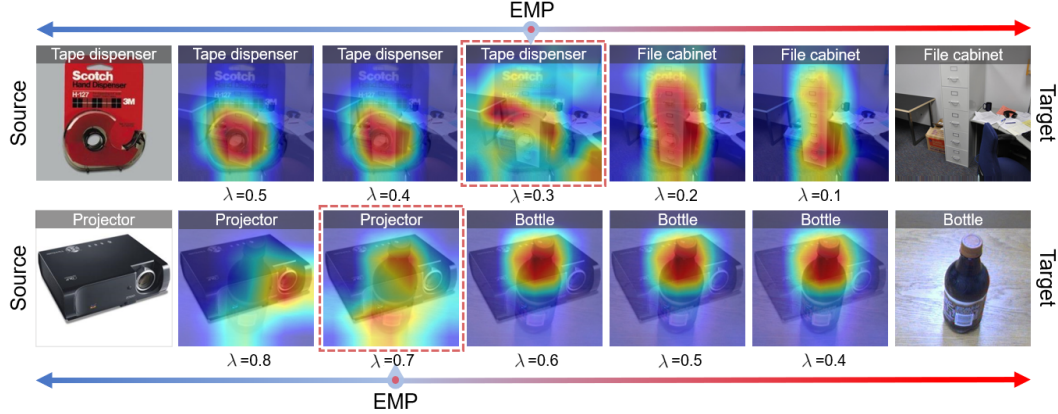


Figure 4. **Grad-CAM visualization.** Our key observations in the vicinal space are as follows: (i) *EMPs* vary depending on the convex combination of instances. (ii) The *top-1* prediction is switched between the source and target labels (e.g., Tape dispenser \leftrightarrow File cabinet) around the EMP. (iii) Grad-CAM highlights the same category as our *top-1* prediction as the most class-discriminative region.

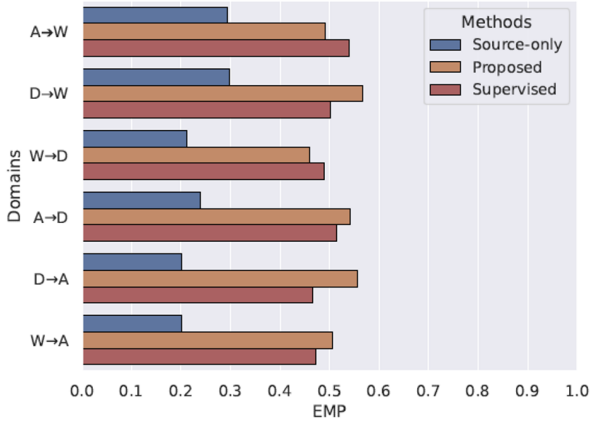


Figure 5. **Equilibrium collapse of labels.** We compare the change of entropy maximization point according to the methods. Before adaptation, the source domain is dominant over the target domain. Contrarily, applying our method equilibrates around 50%, similar to supervised learning.

in an instance; hence, we can identify the most dominant label in each vicinal instance. Now we demonstrate our crucial observations based on the EMP. First, we observe that the EMP is formed differently depending on the convex combinations of the source and target instances. Second, the dominant labels are switched between the source and target labels at the EMP. Lastly, because the EMP is the highest entropy point, Grad-CAM fails to adequately highlight one specific category at this point. We claim that this outcome is due to the uncertainty arising from the confusion between the source and target instances. Furthermore, we discover that the source and target classes are highlighted in instances on both sides of the EMP.

Equilibrium collapse. In Figure 5, we analyze the dominance of labels between the source and target domains. Before adaptation (i.e., source-only), the equilibrium of the label is broken by the dominant-source and recessive-target

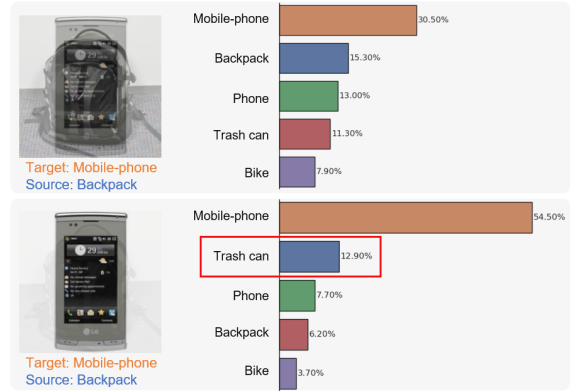


Figure 6. **Predictions in the contrastive space vs. consensus space.** **Top:** The first and second prediction labels consist of source and target labels in the contrastive space. **Bottom:** In the consensus space, the second prediction label is not the source label but a label of another category.

domains. In this case, even if the proportion of the target instances in the mixed-up instance is more than 70% (i.e., target-dominant instance), the prediction is determined by the source label (i.e., source-dominant label). By contrast, when we train the source and target domains in a supervised learning manner, their label dominance is balanced at approximately 50%. After applying our adaptation method, the equilibrium is reached at approximately 50%, which is close to the supervised learning method. In other words, the target-dominant instance is predicted as a target label rather than a source label, and the equilibrium collapse of labels is alleviated.

Analysis of the vicinal space. Our method leverages the vicinal spaces by dividing them into a contrastive space and a consensus space. In Figure 6, we observe that the *top-5* predictions of the two spaces have different characteristics. In the contrastive space, the *top-2* predictions consist of the target label (i.e., mobile phone) and source label (i.e., back-

<i>Baseline</i>	\mathcal{R}_{emp}	\mathcal{R}_{ct}	\mathcal{R}_{cs}	A→W	D→W	W→D	A→D	D→A	W→A	Avg
✓				91.3	98.9	100.0	90.4	72.7	65.6	86.5
✓	✓			95.9	99.1	100.0	95.6	76.3	75.4	90.4
✓	✓	✓		97.1	99.2	100.0	97.2	76.4	76.4	91.1
✓	✓	✓	✓	97.6	99.3	100.0	98.0	77.5	78.4	91.8

Table 4. Ablation results (%) of investigating the effects of our components on Office-31.

Method	C,S,P→A	A,S,P→C	A,C,P→S	A,C,S→P	Avg
MSTN* (Baseline) [48]	85.5	86.22	80.81	95.27	86.95
JiGen (CVPR'19) [4]	86.1	87.6	73.4	98.3	86.3
Meta-MCD (ECCV'20) [23]	87.4	86.18	78.26	97.13	87.24
CMSS (ECCV'20) [51]	88.6	90.4	82	96.9	89.5
DSON (ECCV'20) [37]	86.54	88.61	<u>86.93</u>	99.42	90.38
T-SVDNet (ICCV'21) [26]	90.43	90.61	85.49	98.5	91.25
CoVi (Ours)	93.11	93.86	88.06	<u>99.04</u>	93.52

Table 5. Accuracy (%) on PACS for multi-source unsupervised domain adaptation (ResNet-18). The best accuracy is indicated in bold, and the second-best accuracy is underlined. * Reproduced by ourselves.

pack). In other words, the uncertainty between inter-domain categories is the most critical factor in the predictions. By contrast, in the top-2 predictions of the consensus space, the second label is not the source label, but another category (*i.e.*, trash can) in the target domain that looks similar to the target label (*i.e.*, mobile phone). Hence, mitigating the intra-domain confusion of the target domain in the consensus space can be another starting point to improve performance further.

Effect of the components. We conduct ablation studies to investigate the effectiveness for each component of our method in Table 4. We observe that our *EMP-Mixup* improves the accuracy by an average of 3.9% compared to the baseline [48]. In addition, our contrastive loss shows a significant improvement in tasks A→W and A→D. Meanwhile, in tasks of D→A and W→A, our label-consensus loss has a significant impact on the performance gain. Overall, our proposed method improves the baseline by an average of 5.3%. This experiment verifies that each component contributes positively to performance improvement.

Multi-source domain adaptation. To demonstrate the generality of our instance-wise approach, we experiment with a multi-source domain adaptation task, as shown in Table 5. Our method achieves a performance improvement of over 6% on the PACS dataset compared to the baseline MSTN [48]. In terms of the average accuracy, our method shows a significant performance improvement compared to the state-of-the-art methods. In particular, our method outperforms in three out of four tasks compared with the recent methods.

Feature visualization. We visualize the embedded features on task A→D of the Office-31 dataset using t-SNE [43] in Figure 7. For the baseline MSTN [48] results, we observe that, unlike the source features, the target features do not form cohesive clusters. By contrast, in

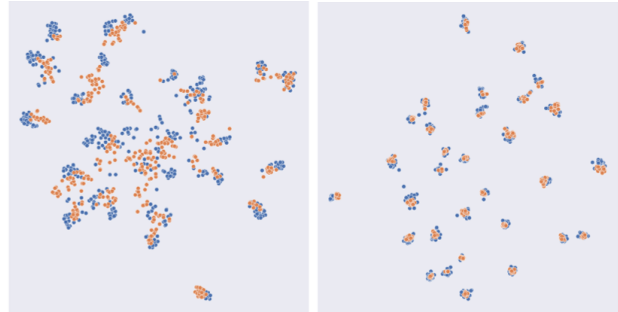


Figure 7. **t-SNE visualization.** Visualization of embedded features on task A→D. Blue and orange points denote the source and target domains, respectively.

our method, the target features organize compact clusters comparable to the source features. These results prove that our method works successfully in the unsupervised domain adaptation task.

5. Conclusions

In this study, we investigate the vicinal space between the source and target domains from the perspective of self-training. We raise the problem of the equilibrium collapse of labels and propose three novel approaches. Our *EMP-Mixup* efficiently minimizes the worst-case risk in the vicinal space. In addition, we reduce inter-domain and intra-domain confusions by dividing the vicinal space into contrastive and consensus space. The competitiveness of our approach suggests that self-predictions in vicinal space can play an important role in solving the UDA problem. We hope that our work will serve as a useful step in alleviating the domain shift problem.

References

- [1] D. Berthelot, N. Carlini, E. D. Cubuk, A. Kurakin, K. Sohn, H. Zhang, and C. Raffel. Remixmatch: Semi-supervised learning with distribution alignment and augmentation anchoring. *arXiv preprint arXiv:1911.09785*, 2019. 2
- [2] D. Berthelot, N. Carlini, I. Goodfellow, N. Papernot, A. Oliver, and C. Raffel. Mixmatch: A holistic approach to semi-supervised learning. *arXiv preprint arXiv:1905.02249*, 2019. 2
- [3] K. Bousmalis, G. Trigeorgis, N. Silberman, D. Krishnan, and D. Erhan. Domain separation networks. *Advances in neural information processing systems*, 29:343–351, 2016. 1

- [4] F. M. Carlucci, A. D’Innocente, S. Bucci, B. Caputo, and T. Tommasi. Domain generalization by solving jigsaw puzzles. In *Proceedings of the IEEE/CVF Conference on Computer Vision and Pattern Recognition*, pages 2229–2238, 2019. 8
- [5] W.-G. Chang, T. You, S. Seo, S. Kwak, and B. Han. Domain-specific batch normalization for unsupervised domain adaptation. In *Proceedings of the IEEE/CVF Conference on Computer Vision and Pattern Recognition*, pages 7354–7362, 2019. 2, 6
- [6] W.-L. Chang, H.-P. Wang, W.-H. Peng, and W.-C. Chiu. All about structure: Adapting structural information across domains for boosting semantic segmentation. In *Proceedings of the IEEE/CVF Conference on Computer Vision and Pattern Recognition*, pages 1900–1909, 2019. 1
- [7] O. Chapelle, J. Weston, L. Bottou, and V. Vapnik. Vicinal risk minimization. *Advances in neural information processing systems*, pages 416–422, 2001. 3
- [8] S. Cui, S. Wang, J. Zhuo, C. Su, Q. Huang, and Q. Tian. Gradually vanishing bridge for adversarial domain adaptation. In *Proceedings of the IEEE/CVF Conference on Computer Vision and Pattern Recognition*, pages 12455–12464, 2020. 1, 6
- [9] Z. Du, J. Li, H. Su, L. Zhu, and K. Lu. Cross-domain gradient discrepancy minimization for unsupervised domain adaptation. In *Proceedings of the IEEE/CVF Conference on Computer Vision and Pattern Recognition*, pages 3937–3946, 2021. 6
- [10] K. Fan. Minimax theorems. *Proceedings of the National Academy of Sciences of the United States of America*, 39(1):42, 1953. 2, 4
- [11] Y. Ganin and V. Lempitsky. Unsupervised domain adaptation by backpropagation. In *International conference on machine learning*, pages 1180–1189. PMLR, 2015. 2, 5
- [12] Y. Ganin, E. Ustinova, H. Ajakan, P. Germain, H. Larochelle, F. Laviolette, M. Marchand, and V. Lempitsky. Domain-adversarial training of neural networks. *The journal of machine learning research*, 17(1):2096–2030, 2016. 2, 5
- [13] R. Gong, W. Li, Y. Chen, and L. V. Gool. Dlow: Domain flow for adaptation and generalization. In *Proceedings of the IEEE/CVF Conference on Computer Vision and Pattern Recognition*, pages 2477–2486, 2019. 1
- [14] I. Goodfellow, J. Pouget-Abadie, M. Mirza, B. Xu, D. Warde-Farley, S. Ozair, A. Courville, and Y. Bengio. Generative adversarial nets. *Advances in neural information processing systems*, 27, 2014. 1, 4
- [15] X. Gu, J. Sun, and Z. Xu. Spherical space domain adaptation with robust pseudo-label loss. In *Proceedings of the IEEE/CVF Conference on Computer Vision and Pattern Recognition*, pages 9101–9110, 2020. 1, 2, 6
- [16] H. Guo, Y. Mao, and R. Zhang. Mixup as locally linear out-of-manifold regularization. In *Proceedings of the AAAI Conference on Artificial Intelligence*, volume 33, pages 3714–3722, 2019. 3
- [17] K. He, X. Zhang, S. Ren, and J. Sun. Deep residual learning for image recognition. In *Proceedings of the IEEE conference on computer vision and pattern recognition*, pages 770–778, 2016. 5
- [18] K. He, X. Zhang, S. Ren, and J. Sun. Identity mappings in deep residual networks. In *European conference on computer vision*, pages 630–645. Springer, 2016. 5
- [19] L. Hu, M. Kan, S. Shan, and X. Chen. Unsupervised domain adaptation with hierarchical gradient synchronization. In *Proceedings of the IEEE/CVF Conference on Computer Vision and Pattern Recognition*, pages 4043–4052, 2020. 6
- [20] Y. Jin, X. Wang, M. Long, and J. Wang. Minimum class confusion for versatile domain adaptation. In *European Conference on Computer Vision*, pages 464–480. Springer, 2020. 6
- [21] G. Kang, L. Jiang, Y. Yang, and A. G. Hauptmann. Contrastive adaptation network for unsupervised domain adaptation. In *Proceedings of the IEEE/CVF Conference on Computer Vision and Pattern Recognition*, pages 4893–4902, 2019. 2, 6
- [22] D.-H. Lee et al. Pseudo-label: The simple and efficient semi-supervised learning method for deep neural networks. In *Workshop on challenges in representation learning, ICML*, volume 3, page 896, 2013. 1, 2
- [23] D. Li and T. Hospedales. Online meta-learning for multi-source and semi-supervised domain adaptation. In *European Conference on Computer Vision*, pages 382–403. Springer, 2020. 8
- [24] D. Li, Y. Yang, Y.-Z. Song, and T. M. Hospedales. Deeper, broader and artier domain generalization. In *Proceedings of the IEEE international conference on computer vision*, pages 5542–5550, 2017. 2, 5
- [25] M. Li, Y.-M. Zhai, Y.-W. Luo, P.-F. Ge, and C.-X. Ren. Enhanced transport distance for unsupervised domain adaptation. In *Proceedings of the IEEE/CVF Conference on Computer Vision and Pattern Recognition*, pages 13936–13944, 2020. 6
- [26] R. Li, X. Jia, J. He, S. Chen, and Q. Hu. T-svdnet: Exploring high-order prototypical correlations for multi-source domain adaptation. In *Proceedings of the IEEE/CVF International Conference on Computer Vision*, pages 9991–10000, 2021. 8
- [27] Z. Lu, Y. Yang, X. Zhu, C. Liu, Y.-Z. Song, and T. Xiang. Stochastic classifiers for unsupervised domain adaptation. In *Proceedings of the IEEE/CVF Conference on Computer Vision and Pattern Recognition*, pages 9111–9120, 2020. 6
- [28] Z. Mai, G. Hu, D. Chen, F. Shen, and H. T. Shen. Metamixup: Learning adaptive interpolation policy of mixup with metalearning. *IEEE Transactions on Neural Networks and Learning Systems*, 2021. 3
- [29] T. Miyato, S.-i. Maeda, M. Koyama, and S. Ishii. Virtual adversarial training: a regularization method for supervised and semi-supervised learning. *IEEE transactions on pattern analysis and machine intelligence*, 41(8):1979–1993, 2018. 4
- [30] J. Na, H. Jung, H. J. Chang, and W. Hwang. Fixbi: Bridging domain spaces for unsupervised domain adaptation. In *Proceedings of the IEEE/CVF Conference on Computer Vision and Pattern Recognition*, pages 1094–1103, 2021. 1, 2, 3, 5, 6
- [31] F. Pan, I. Shin, F. Rameau, S. Lee, and I. S. Kweon. Unsupervised intra-domain adaptation for semantic segmentation

- through self-supervision. In *Proceedings of the IEEE/CVF Conference on Computer Vision and Pattern Recognition*, pages 3764–3773, 2020. 2
- [32] X. Peng, B. Usman, N. Kaushik, J. Hoffman, D. Wang, and K. Saenko. Visda: The visual domain adaptation challenge. *arXiv preprint arXiv:1710.06924*, 2017. 2, 5
- [33] H. Pham, Z. Dai, Q. Xie, and Q. V. Le. Meta pseudo labels. In *Proceedings of the IEEE/CVF Conference on Computer Vision and Pattern Recognition*, pages 11557–11568, 2021. 1
- [34] K. Saenko, B. Kulis, M. Fritz, and T. Darrell. Adapting visual category models to new domains. In *European conference on computer vision*, pages 213–226. Springer, 2010. 2, 5
- [35] K. Saito, Y. Ushiku, and T. Harada. Asymmetric tri-training for unsupervised domain adaptation. In *International Conference on Machine Learning*, pages 2988–2997. PMLR, 2017. 1
- [36] R. R. Selvaraju, M. Cogswell, A. Das, R. Vedantam, D. Parikh, and D. Batra. Grad-cam: Visual explanations from deep networks via gradient-based localization. In *Proceedings of the IEEE international conference on computer vision*, pages 618–626, 2017. 6
- [37] S. Seo, Y. Suh, D. Kim, G. Kim, J. Han, and B. Han. Learning to optimize domain specific normalization for domain generalization. In *Computer Vision–ECCV 2020: 16th European Conference, Glasgow, UK, August 23–28, 2020, Proceedings, Part XXII 16*, pages 68–83. Springer, 2020. 8
- [38] A. Sharma, T. Kalluri, and M. Chandraker. Instance level affinity-based transfer for unsupervised domain adaptation. In *Proceedings of the IEEE/CVF Conference on Computer Vision and Pattern Recognition*, pages 5361–5371, 2021. 6
- [39] H. Shimodaira. Improving predictive inference under covariate shift by weighting the log-likelihood function. *Journal of statistical planning and inference*, 90(2):227–244, 2000. 1
- [40] I. Shin, S. Woo, F. Pan, and I. S. Kweon. Two-phase pseudo label densification for self-training based domain adaptation. In *European conference on computer vision*, pages 532–548. Springer, 2020. 1
- [41] K. Sohn, D. Berthelot, C.-L. Li, Z. Zhang, N. Carlini, E. D. Cubuk, A. Kurakin, H. Zhang, and C. Raffel. Fixmatch: Simplifying semi-supervised learning with consistency and confidence. *arXiv preprint arXiv:2001.07685*, 2020. 2
- [42] H. Tang, K. Chen, and K. Jia. Unsupervised domain adaptation via structurally regularized deep clustering. In *Proceedings of the IEEE/CVF conference on computer vision and pattern recognition*, pages 8725–8735, 2020. 6
- [43] L. Van der Maaten and G. Hinton. Visualizing data using t-sne. *Journal of machine learning research*, 9(11), 2008. 8
- [44] H. Venkateswara, J. Eusebio, S. Chakraborty, and S. Panchanathan. Deep hashing network for unsupervised domain adaptation. In *Proceedings of the IEEE conference on computer vision and pattern recognition*, pages 5018–5027, 2017. 2, 5
- [45] G. Wei, C. Lan, W. Zeng, and Z. Chen. Metaalign: Coordinating domain alignment and classification for unsupervised domain adaptation. In *Proceedings of the IEEE/CVF Conference on Computer Vision and Pattern Recognition*, pages 16643–16653, 2021. 6
- [46] Y. Wu, D. Inkpen, and A. El-Roby. Dual mixup regularized learning for adversarial domain adaptation. In *European Conference on Computer Vision*, pages 540–555. Springer, 2020. 1, 2, 6
- [47] N. Xiao and L. Zhang. Dynamic weighted learning for unsupervised domain adaptation. In *Proceedings of the IEEE/CVF Conference on Computer Vision and Pattern Recognition*, pages 15242–15251, 2021. 1, 6
- [48] S. Xie, Z. Zheng, L. Chen, and C. Chen. Learning semantic representations for unsupervised domain adaptation. In *International conference on machine learning*, pages 5423–5432. PMLR, 2018. 2, 6, 8
- [49] M. Xu, J. Zhang, B. Ni, T. Li, C. Wang, Q. Tian, and W. Zhang. Adversarial domain adaptation with domain mixup. In *Proceedings of the AAAI Conference on Artificial Intelligence*, volume 34, pages 6502–6509, 2020. 1, 2
- [50] J. Yang, H. Zou, Y. Zhou, Z. Zeng, and L. Xie. Mind the discriminability: Asymmetric adversarial domain adaptation. In *European Conference on Computer Vision*, pages 589–606. Springer, 2020. 6
- [51] L. Yang, Y. Balaji, S.-N. Lim, and A. Shrivastava. Curriculum manager for source selection in multi-source domain adaptation. In *Computer Vision–ECCV 2020: 16th European Conference, Glasgow, UK, August 23–28, 2020, Proceedings, Part XIV 16*, pages 608–624. Springer, 2020. 8
- [52] Z. Yue, Q. Sun, X.-S. Hua, and H. Zhang. Transporting causal mechanisms for unsupervised domain adaptation. In *Proceedings of the IEEE/CVF International Conference on Computer Vision*, pages 8599–8608, 2021. 1, 6
- [53] H. Zhang, M. Cisse, Y. N. Dauphin, and D. Lopez-Paz. mixup: Beyond empirical risk minimization. *arXiv preprint arXiv:1710.09412*, 2017. 1, 2, 3, 6
- [54] J. Zhu, L. Shi, J. Yan, and H. Zha. Automix: Mixup networks for sample interpolation via cooperative barycenter learning. In *European Conference on Computer Vision*, pages 633–649. Springer, 2020. 3